International Journal of scientific research and management (IJSRM)
||Volume||1||Issue|| 3 ||Pages|| 112-132 ||2013||
Website: www.ijsrm.in ISSN (e): 2321-3418

GEOELECTRIC DETERMINATION OF THE GROUNDWATER POTENTIAL OF PARTS OF POMPO VILLAGE, MINNA, NIGERIA

Chikwelu, E. E., and Udensi, E. E.

Department of Physics, Federal University of Technology, Minna. (chikwelubright@gmail.com)

Abstract: The Geoelectric determination of groundwater potential of parts of Pompo village opposite Federal University of Technology, Gidan Kwano Campus, Minna, was carried out using conventional Vertical Electrical Sounding (VES) and Self potential methods. The aim of this survey is to determining the ground water potential of the area and to locate those areas that could be useful for civil engineering workers. The data obtained were interpreted using computer-based program called Zohdy, which showed a laterally and vertical varying succession of high and low resistive geoelectric layers throughout the area. The resulting (Interpreted) models were used to produce regolith map and self potential contour maps. The aquifer system of the study area is generally characterized by relatively low resistivity value between 374Ωm and about 1800Ωm in the weathered basement and supported on some VES points by fractured basement and its thickness ranges from 3m to >20m. The most promising region of the site lies on west and south-eastern part, while the civil and the environmental works will be best located at the northern and southern part where the fresh basement is uplifted.

Keywords: Groundwater, Vertical Electrical Sounding, Self potential, Regolith, Portable water, Geologic structure, Geoelectric, Determination.

Introduction

Groundwater is the largest available reservoir of fresh water. A majority of fresh water is locked away as ice in the polar ice caps, continent ice sheets and glaciers beneath the ground. Water in rivers and lakes only account for less than 1% of the Worlds' fresh water reserves (Dogara. 1995). It is among natural resources bestow the human race. There must be space between the rock particles for groundwater to flow and the Earth's material becomes denser with more depth. Essentially, the weights of the rock above condense the rock below and squeeze out to open the pore spaces deeper in the Earth. That is why groundwater can only be found within a few kilometers of the Earth's surface. Observation shows that groundwater comes from rain, snow, sheet and hail that soak into the ground and become the groundwater responsible for the spring, wells and bore holes (Salako, et al., 2005) Groundwater is water located beneath the ground surface in soil pore spaces and in the fractures of lithologic formations. A unit of rock or an unconsolidated deposit is called an aquifer when it can yield a usable quantity of water (Udensi, 2005). The depth at which soil pore spaces or fractures and voids in rock become completely saturated with water is called water table.

The development of the community is imminent because the relocation of the university to this area will necessarily bring about the influx of population to the area within a foreseeable future. There is therefore, the need for a scientific identification of parameters governing groundwater resources, assessment and management, particularly if satisfactory living conditions of the inhabitants are to be catered for and to delineate the areas that would be suitable for possible civil engineering and environmental development.

The Vertical Electric Sounding (VES) has been the most important geophysical method of water prospecting in areas of deep in situ weathering of fresh bedrock. Hence, it has been chosen for this work because it has proven to be an economic, quick and effective means of solving most groundwater problems in different parts of the world. The thickness of the overburden can also be estimated using VES method as presented in this work.

Study Area Description.

The study area is located in Pompo village close to Minna in Niger State, (Figure 1) Pompo village is located between km 12 and 13 along Minna-Kateregi-Bida road on the opposite side of the Gidan Kwano Campus of Federal University of Technology (F.U.T) Minna, (Figure 2). The study area is located between latitude $9^0$31'N and $9^0$32'N and longitude $6^0$28'E to $6^0$29'E in a part of Minna SW sheet 42. The investigated site is a square of 500m by

500m, covering an area of 250,000 m^2. It is about 30m away from the major road (Minna- Keteregi- Bida road), 500m beginning from latitude $9^0 31$'N and 500m eastward from the start point.

The rock types found in the study area consists predominantly of coarse-grained biotite granite and granodiorite. The granite types and the granodiorite together form part of the older Granite. The result of the borehole log and hand-dug wells from the area show that the area has a good potential for ground water development. The Basement Complex of Africa is a heterogeneous mixture of crystalline rocks, predominantly of a granitic or gneissose character. Groundwater occurs within these crystalline rocks in fractured or in the superficial weathered zones.

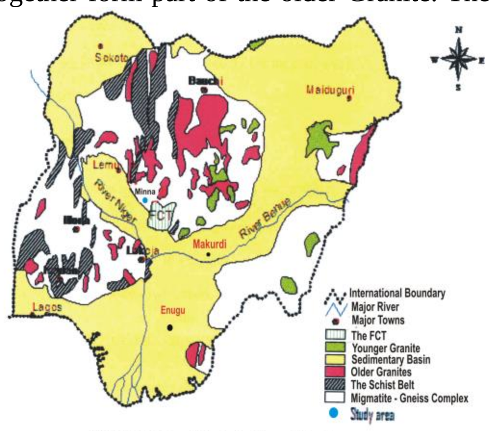

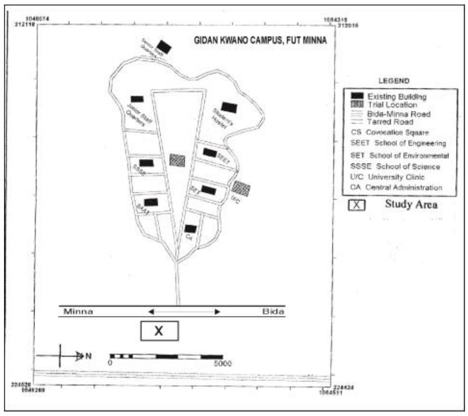

Figure 1 and 2: General Geology Map of Nigeria showing the location of Minna (Study Area) and Map of Federal University of Technology, Gidan Kwano Campus Minna showing the location and accessibility of the study area.

Experiment/tests conducted

The study area was inspected and gridded as shown in Figure 3. Thirty-six (36) numbers of VES points were covered. The Terrameter SAS-4000 was the instrument uses and is capable of operating in different modes: Resistivity, Self-potential and Induced Polarization, was used. However, electrical resistivity and self potential data were collected using VES (Schlumberger).

Results and Discussion

The interpretation was done using an iterative computer program called the Zohdy graphical method. This program performs automatic interpretation of the Schlumberger sounding curves. This curve gives the equivalent n-layer model from the apparent resistivity of each sounding. Further analyses of the interpreted VES data (Zohdy) were done using Surfer 8 and Minitab 14 to get deeper information of the subsurface.

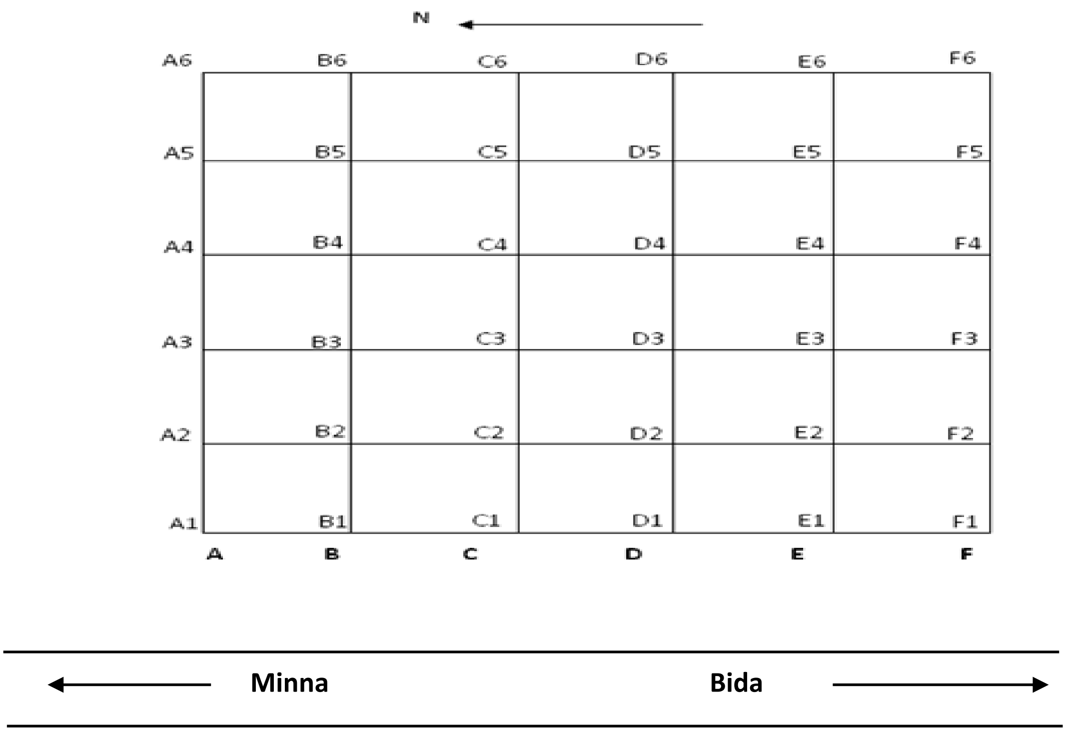

Figure 3: The profile layout for VES data collection N-S (North-South).

A continuous variation of resistivity with depth curve is easily derived from the multi-layer step function curve by drawing a curve that passes through the logarithmic mid-point of each vertical and horizontal line on the multi-step function model. This was used to construct.

i. Regolith contour map
ii. Self potential contour map.

Geoelectric Section

From the digitized Zohdy curves shown under the Appendix A the following deductions can be made. These digitized data were summarized in Table form; the tables were obtained through average of similar resistivity values that span through several depths. Both the resistivity values and their corresponding depths were averaged. The difference between successive depths gives the thickness of a layer while the resistivity values (averaged) correspond to the resistivity of that particular layer. The depth column indicates the beginning of a layer. These processes were repeated for the 36 VES points. Table 1-6 are the summary of the analysis of the VES geoelectric sections.

Profile A

Table 1 shows the summary of the VES interpretation for profile A. The whole profile can be interpreted as three layer model VES A_1 and VES A_3 which indicate four-layer models. The profile shows HQ and H resistivity type curves. The following could be deduced:

- The first layer has resistivity values ranging from 73.65 Ωm to 556.81 Ωm. The highest resistivity value of 556.81 Ωm is found at VES A_1 and the lowest resistivity value of 73.65 Ωm is at VES A_6. The layer is thickest at VES A_5 (about 1.05m) and thinnest at VES A_3 (about 0.54 m).
- The second layer has resistivity values ranging between 40.28 Ωm to 294.21 Ωm. The highest resistivity value of this layer is found at VES A_1 (about 294.21 Ωm) while the lowest resistivity value is found at VES A_6 (about 40.28Ωm). The layer is thickest at VES A_5 (about 14.32m) and thinnest at VES A_3 (about 1.97m).The small pocket of low resistivity material overlies the third layer A_1 and A_3. It has resistivity values ranging between 63.54 Ωm to 217.87 Ωm. The highest resistivity value of 217.87 Ωm is found at A_1 while the lowest resistivity value of 63.54 Ωm is found at A_3.
- The third layer has resistivity values ranging between 185.79 Ωm to 1682.37 Ωm. The highest resistivity value of 1682.37 Ωm is found at VES A_5 and the lowest resistivity value of 185.79 Ωm is found at VES A_3. This layer is deepest at VES A_1 and A_5, shallowest at VES A_2.

Table 1 VES Interpretation of Profile A

VES PT	No of Layers	Type of layer curve	Average Resistivity (Ωm)	Layer thickness (m)	Depth (m)
A_1	1	HQ	556.81	0.71	0.00
	2		294.21	4.15	0.71
	3		217.87	10.51	4.86
	4		1052.72	∞	15.37
A_2	1	H	83.61	0.58	0.00
	2		60.06	5.20	0.58
	3		870.80	∞	5.78
A_3	1	HQ	364.15	0.54	0.00
	2		70.81	1.97	0.54
	3		63.54	5.42	2.51
	4		185.79	∞	7.93
A_4	1	H	384.54	0.94	0.00
	2		96.72	12.89	0.94
	3		1354.09	∞	13.83
A_5	1	H	208.49	1.05	0.00
	2		72.44	14.32	1.05
	3		1682.37	∞	15.37
A_6	1	H	73.65	0.64	0.00
	2		40.28	13.19	0.64
	3		1137.67	∞	13.83

Profile B

Table 2 shows the summary of the VES interpretation of profile B. The whole profile can be summarized into three layers with H and A type curves. The following could be deduced:

- The first layer has resistivity values ranging from 4.26 Ωm to 255.31 Ωm. The highest resistivity value of 255.31 Ωm is found at VES B_1 and the lowest resistivity value of 4.26 Ωm is at VES B_5. The layer is thickest at VES B_1 (about 0.94m) and thinnest at VES B_4 (about 0.39 m).
- The second layer has resistivity values ranging between 14.76 Ωm to 114.27 Ωm. The highest resistivity value of this layer is found at VES B_1 (about 114.27 Ωm and lowest resistivity value of 14.76 Ωm is found at VES B_3. The layer is thickest at VES B_6 (about 13.19m) and thinnest at VES B_3 (about 5.20m).
- The third layer has resistivity values ranging between 653.96 Ωm to 1724.53 Ωm. The highest resistivity value of 1724.53 Ωm is found at VES B_5 and the lowest resistivity value of 653.96 Ωm is found at VES B_6. This layer is deep at VES B_1 and B_6, shallow at VES B_2, B_3 and B_4

Table 2 VES Interpretation of Profile B

VES PT	No of Layers	Type of layer curve	Average Resistivity (Ωm)	Layer thickness (m)	Depth (m)
B_1	1	H	255.31	0.94	0.00
	2		114.27	12.89	0.94
	3		759.74	∞	13.83
B_2	1	H	42.87	0.53	0.00
	2		36.17	5.25	0.53
	3		900.59	∞	5.78
B_3	1	H	18.88	0.58	0.00
	2		14.76	5.20	0.58
	3		1003.83	∞	5.78
B_4	1	H	56.36	0.39	0.00
	2		46.70	5.39	0.39
	3		1123.33	∞	5.78
B_5	1	A	4.26	0.47	0.00
	2		63.56	9.61	0.47
	3		1724.53	∞	10.08
B_6	1	H	76.04	0.64	0.00
	2		54.04	13.19	0.64
	3		653.96	∞	13.83

Profile C

Table 3 shows the summary of the VES interpretation of profile C. The whole profile can be summarized into three layers with H type curves. The following could be deduced:

- The first layer has resistivity values ranging from 2.83 Ωm to 135.06 Ωm. The highest resistivity value of 135.06 Ωm is found at VES C_2 and the lowest resistivity value of 2.83 Ωm is at VES C_6. The layer is thickest at VES C_4 (about 1.05m) and thinnest at VES C_1 (about 0.39 m).
- The second layer has resistivity values ranging between 2.53 Ωm to 88.31 Ωm. The highest resistivity value of this layer is found at VES C_1 (about 88.31 Ωm) and lowest resistivity value of 2.53 Ωm is found at VES C_6. The layer is thickest at VES C_1 about 17.88m and thinnest at VES C_3 about 5.78m.
- The third layer has resistivity values ranging between 143.13 Ωm to 2126.22 Ωm. The highest resistivity value of 2126.22 Ωm is found at VES C_2 and the lowest resistivity value of 143.13 Ωm is found at VES C_6. This layer is deepest at VES C_1 and shallowest at VES C_3.

Table 3 VES Interpretation of Profile C

VES PT	No of Layers	Type of layer curve	Average Resistivity (Ωm)	Layer thickness (m)	Depth (m)
C_1	1	H	114.00	0.39	0.00
	2		88.31	17.88	0.39
	3		1852.02	∞	18.27
C_2	1	H	135.06	0.64	0.00
	2		80.75	8.78	0.64
	3		2126.22	∞	9.42
C_3	1	H	59.24	0.64	0.00
	2		48.23	5.78	0.64
	3		1556.69	∞	6.42
C_4	1	H	112.32	1.05	0.00
	2		60.34	9.42	1.05
	3		930.27	∞	10.47
C_5	1	H	15.13	0.58	0.00
	2		45.85	7.90	0.58
	3		1382.87	∞	8.48
C_6	1	H	2.83	0.71	0.00
	2		2.53	6.42	0.71
	3		143.13	∞	7.13

Profile D

Table 4 shows the summary of the VES interpretation of profile D. The whole profile can be summarized into three layers with H type curves. The following could be deduced:

- The first layer has resistivity values ranging from 40.24Ωm to 194.14Ωm. The highest resistivity value of 194.14 Ωm is found at VES D_4 and the lowest resistivity value of 4O.24 Ωm is at VES D_3. The layer is thickest at VES D_2 (about 0.94m) and thinnest at VES D_3 (about 0.39 m).
- The second layer has resistivity values ranging between 32.01 Ωm to 138.20 Ωm. The highest resistivity value of this layer is found at VES D_4 (about 138.20 Ωm and lowest resistivity value of 32.01 Ωm is found at VES D_6. The layer is thickest at VES D_2 about 12.89m and thinnest at VES D_3 about 5.39m.
- The third layer has resistivity values ranging between 399.25 Ωm to 1401.71 Ωm. The highest resistivity value of 1401.71 Ωm is found at VES D_1 and the lowest resistivity value of 399.25 Ωm is found at VES D_5. This layer is deepest at VES D_2 and shallowest at VES D_3.

•

Table 4 VES Interpretation of Profile D

VES PT	No of Layers	Type of layer curve	Average Resistivity (Ωm)	Layer thickness (m)	Depth (m)
D_1	1	H	58.34	0.64	0.00
	2		46.81	8.78	0.64
	3		1401.71	∞	9.42
D_2	1	H	77.90	0.94	0.00
	2		73.40	12.89	0.94
	3		1052.66	∞	13.83
D_3	1	H	40.24	0.39	0.00
	2		36.790	5.39	0.38
	3		533.56	∞	5.78
D_4	1	H	194.14	0.64	0.00
	2		138.20	8.78	064
	3		1069.04	∞	9.42
D_5	1	H	83.76	0.85	0.00
	2		41.78	7.63	0.85
	3		399.25	∞	8.48
D_6	1	H	67.43	0.64	0.00
	2		32.01	8.78	0.64
	3		615.74	∞	9.42

Profile E

Table 1.5 shows the summary of the VES interpretation of profile E. The whole profile can be summarized into three layers with H type curves. The following be inferred:

- The first layer has resistivity values ranging from 35.09 Ωm to 154.82 Ωm. The highest resistivity value of 154.82 Ωm is found at VES E_6 and the lowest resistivity value of 35.09 Ωm is at VES E_1. The layer is thickest at VES E_2 (about 0.79m) and thinnest at VES E_3 (about 0.44m).
- The second layer has resistivity values ranging between 19.20 Ωm to 73.15 Ωm. The highest resistivity value of this layer is found at VES E_6 (about 73.15 Ωm and lowest resistivity value of 19.20 Ωm is found at VES E_5. The layer is thickest at VES E_6 about 19.66m and thinnest at VES E_1 about 3.36m.
- The third layer has resistivity values ranging between 373.60 Ωm to 4176.25 Ωm. The highest resistivity value of 4176.25 Ωm is found at VES E_2 and the lowest resistivity value of 373.60 Ωm is found at VES E_1. This layer is deepest at VES E_6 and shallowest at VES E_1.

Table 5 VES Interpretation of Profile E

VES PT	No of Layers	Type of layer curve	Average Resistivity (Ωm)	Layer thickness (m)	Depth (m)
E_1	1	H	35.09	0.58	0.00
	2		31.32	3.36	0.54
	3		373.60	∞	3.94
E_2	1	H	43.21	0.79	0.00
	2		32.53	4.61	0.79
	3		4176.25	∞	5.40
E_3	1	H	45.87	0.44	0.00
	2		34.90	5.98	0.44
	3		516.98	∞	6.42
E_4	1	H	47.02	0.44	0.00
	2		44.99	5.98	0.44
	3		2495.41	∞	6.42
E_5	1	H	37.74	0.58	0.00
	2		19.20	7.90	0.58
	3		822.96	∞	8.48
E_6	1	H	154.82	0.64	0.00
	2		73.15	19.66	0.64
	3		1513.03	∞	20.30

Profile F

Table 6 shows the summary of the VES interpretation of profile F. The whole profile can be summarized into three layers with H type curves.

- The first layer has resistivity values ranging from 43.69Ωm to 211.94Ωm. The highest resistivity value of 211.94 Ωm is found at VES F_3 and the lowest resistivity value of 43.69 Ωm is at VES F_2. The layer is thickest at VES F_6 (about 1.38m) and thinnest at VES F_2 (about 0.39 m).
- The second layer has resistivity values ranging between 26.97 Ωm to 98.01 Ωm. The highest resistivity value of this layer is found at VES F_3 (about 98.01 Ωm and lowest resistivity value of 26.97 Ωm is found at VES F_2. The layer is thickest at VES F_1 about 13.19m and thinnest at VES F_4 about 2.10m.
- The third layer has resistivity values ranging between 676.24 Ωm to 2476.94 Ωm. The highest resistivity value of 2476.94 Ωm is found at VES F_2 and the lowest resistivity value of 676.24 Ωm is found at VES F_1. This layer is deepest at VES F_6 and shallowest at VES F_4.

Table 6 VES Interpretation of Profile F

VES PT	No of Layers	Type of layer curve	Average Resistivity (Ωm)	Layer thickness (m)	Depth (m)
F_1	1	H	118.11	0.64	0.00
	2		56.75	13.19	0.64
	3		676.24	∞	13.83
F_2	1	H	43.69	0.39	0.00
	2		26.97	5.39	0.39
	3		2476.94	∞	5.78
F_3	1	H	211.94	0.64	0.00
	2		98.01	5.78	0.64
	3		1246.50	∞	6.42
F_4	1	H	87.96	0.58	0.00
	2		51.58	2.10	0.58
	3		1141.91	∞	2.68
F_5	1	H	65.05	0.94	0.00
	2		36.84	12.89	0.94
	3		910.33	∞	13.83
F_6	1	H	100.22	1.38	0.00
	2		65.46	12.50	1.38
	3		1155.67	∞	13.88

Regolith contour map: The regolith consists of the collapsed zone and the saprolite, and varies in thickness from less than a meter to as much as 35m. This is usually subdivided into an upper and lower saprolite relative to current (or previous) water levels, in addition to sometimes a basal breciated zone where rock fragmentation is largely unaccompanied by mineralogical changes. The water table occurs typically at shallow depth and the weathered aquifer provides the main storage for deep boreholes as well as both storage and transmissivity for wells and shallow boreholes. The depth and intensity of weathering of the regolith is not necessarily a measure of its usefulness as an aquifer (Ajibade A. C 1976).

Saprolite is derived from institu weathering and is desegregated. An upper saprolite may be distinguished by higher proportions of the more advanced secondary clay minerals (kaolinite): the lower saprolite has a greater abundance of primary minerals combined with the earlier forms of secondary clay minerals. The boundary with the underlying saprock may be sharp (against coarser-grained massive rock) or transitional (against banded or fine-grained rocks) (Kearey, et al 2002).

The contour plot of regolith thickness is as shown in Figure 3. It is contoured at interval of 3m. The data used to produce this map were obtained from the Zohdy interpretation. The depth values corresponding to the regolith overburden aquifer layer of the entire (36) VES points. Western and south-east parts of the study area constitute a wide size for ground water collection. The central portion along the north-south line is shallow.

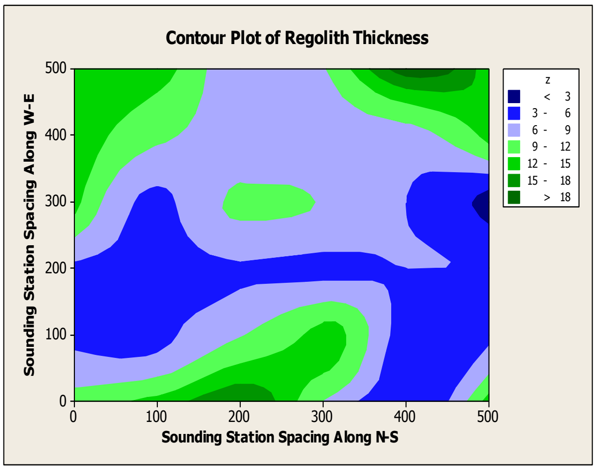

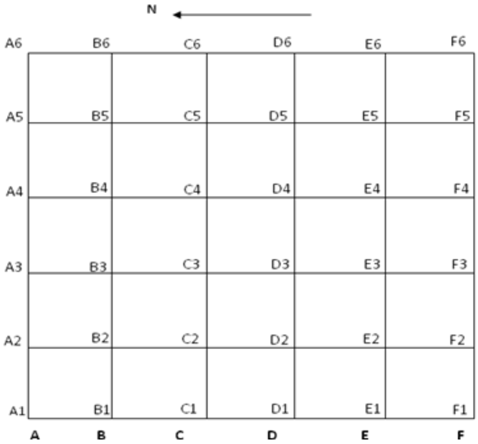

Figure 3: Contour Plot of Regolith Thickness.

The Self-Potential (sp) contour map: Self Potential (SP) geophysical surveys measure the difference in potential between any two points on the ground produced by small, naturally produced currents that occur beneath the Earth's surface. The SP method is passive, non-intrusive and does not require the application of an electric current. Small potentials of the order of a few millivolts are produced by two electrolytic solutions of differing concentrations that are in direct contact, and by the flow of electrolytic fluids through porous materials (streaming potential). Larger ground potentials are produced by conductive mineralised ore bodies partially immersed below the water table.

Figures 4 and 5 present the contour trend of the SP contour maps. Positive SP value within the range of 10mV-100mV is an indication of a water bearing formation (Salako and Udensi, 2005). The southeast and western part happens to be the major points with positive SP, hence a good site for borehole drilling. Nevertheless, some part of the southeast (VES A4, A6, B3-B6) are not in agreement. Regions of negative SP most likely indicate the presence of some form of minerals. This will require further investigation.

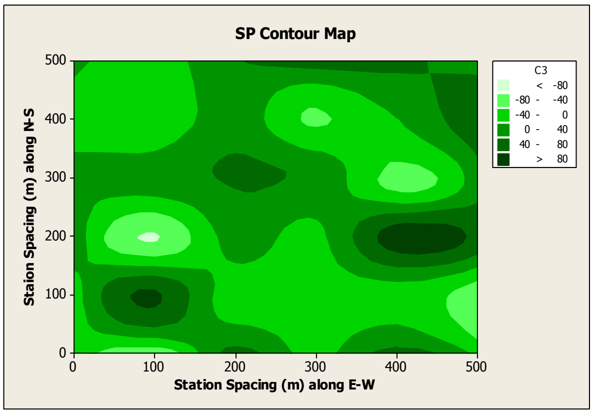

Figure 4 SP Contour Map (Minitab 14)

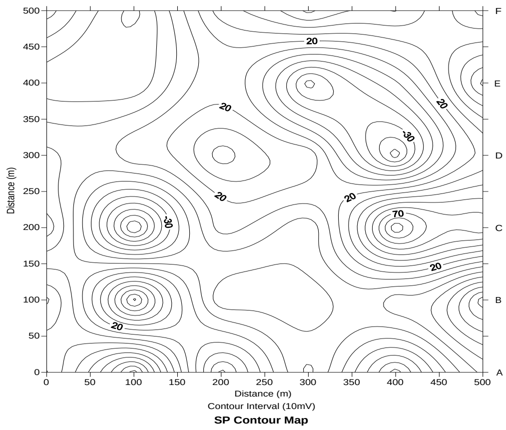

Figure 5 SP Contour Map (Surfer 8)

Conclusion

In other to achieve the aims set out for this study, the electrical resistivity method (Vertical electrical sounding, Electrical mapping and Self potential) was used successfully for the determination of suitable areas for groundwater exploitation and the delineation of areas for civil engineering works at low risk. From the VES data, the overburden thickness and the resistivity values of different layers were determined.

The regolith thickness contour map clearly gave indications of the nature of weathered layer with depth and extent of fracture. This further aided the interpretation of areas with good aquifer potential.

The self-potential (SP) contour map corroborates and concretizes the result from vertical electrical sounding and profiling method. An area with very low positive SP (10mV-100mV) implies that the area will be very resourceful for underground water exploitation. This thus agreed to a large extent with electrical resistivity (profiling and VES) data.

Three main factors that determine the areas suitable for groundwater exploitation are:

- **(i) The conductivity of the subsurface:** groundwater will cause an area to be highly conductive and hence low resistivity value; clayey subsurface could equally be highly conductive. Therefore, water (aquifer) could be delineated by further applications of geological controls (Makama et al 1999).
- **(ii) The presence of suitable aquifer** (weathered and fractured basement) and
- **(iii) The thickness of the aquifer**

In a basement complex terrain, groundwater is confined within weathered layer (saprolite), fractured/jointed or sheared basement (saprock) columns (Aboh, 1996). Also, Dogara, (1995), Ajayi and Hassan, (1990), classified aquifer components in the basement areas to be weathered and fractured basement. Thus, where the fractured zone is saturated, relatively high groundwater yield can be obtained from borehole penetrating such a sequence (Adeniyi et al, 1988). The best areas identified as suitable for ground water exploitation are the western and south-east parts of the study area. Similarly, northern and southern parts of the study area are identified as most suitable for civil engineering works.

References

1. Aboh O. H, 1996: A Regional Geophysical Investigation of the Groundwater Potential of Iyara, Ijumu Local Government Area, Kogi State using the Electrical Resistivity and VIF methods. Published M.Sc. Thesis, Almadu Bello University, Zaria.
2. Adeniyi, J. O, Udensi, E. E. and Okosun, E. A., 1988: Site selection Survey for a Seismic Observatory Station using Geological and Geophysical Techniques. Published Report; Pp 1-5.
3. Ajayi, C. O. and Hassan, 1990: The Delineation of the Aquifer Overlying the Basement Complex in the Western part of the Kubanni Basin of Zaria, Nigeria.
4. Ajibade, A. C., 1976: Provisional Classification and Correlation of the Schist Belt in Northwestern Nigeria. Elizabethan Publishing Col, Ibadan, Pp. 85-90.
5. Dogara, M. D., 1995: D. C. Resistivity Investigation of the groundwater potential in Romi, Chikun Local Government, Kaduna State, Nigeria. Published M.Sc. Thesis ABU, Zaria.
6. Golden Software Inc., 2002: Surface Mapping System, Surfer Version 8.01 Golden Software Inc, Golden Colarado 80401-1866.
7. Instruction Manual: ABEM Terrameter SAS 4000/SAS 1000: ABEM Printed Matter No. 93101.
8. Kearey, P., Brooks, M. and Ian, H., 2002: An Introduction to Geophysical Exploration, Third Edition. Blackwell publishing.
9. Makama, B.S. and Shekwolo, P.D (1999). Appropriate Bore Hole Design and Construction in Basement Complex Rocks of Niger State. *Journal of Geology 8*. Pp 4-6.
10. Salako, K A. and Udensi, E. E., 2005: Vertical electrical Sounding Investigation of Western part of the Federal University of Technology Gidan Kwano campus, Minna Ist Annual S.S.S.E Conference F.U.T. Minna Book of reading Vol.1 pp 69-75.
11. Telford, N. W., Geldart, L. P., Sherriff, R. S. and Keys, D. A., 1976: Applied Geophysics, Second Edition, Cambridge University Press, Cambridge.
12. Udensi, E.E., Ogunbanjo, M.I, Nwosu, J.E, Jonah, S.A, Kolo, M.T, Onuduku, U.S, Crown, I.E, Daniyan, M.A, Adeniyi, J.O and Okosun, F.A 2005: Hydrogeological and Geophysical Surveys for ground water at designated premises of the main campus of the Federal University of Technology, Minna; *Zuma*: *Journal of Pure and Applied Science (ZJ PAS)*, Vol.7 (1), pp 52-58.
13. Udensi, E.E., Ojo, S.B and Ajakaiye, D.E (1986). A three dimensional interpretation of the Bouger Anomalies over the Minna Batholith in central Nigeria. Precambrian Res. 32:1-15.
14. Zohdy, A.A.R. and D. B. Jackson, 1989: Schlumberger Sounding data processing and Interpretation (Version 1.88) U.S. Geological Survey, Denver Co.